24th COBEM - 2017

ABCM
Associação Brasileira de Engenharia e Ciências Mecânicas

24th ABCM International Congress of Mechanical Engineering
December 3-8, 2017, Curitiba, PR, Brazil

# COBEM-2017-2358
# WAVE PROPAGATION AND FREQUENCY BAND STRUCTURE IN CYLINDRICAL SHELLS

**F. N. Pereira**
University of Maranhão - UEMA, Mechanical Engineering, Cidade Universitária Paulo VI, s/n, São Luís - MA, CEP65055-310
flaviomecn@yahoo.com.br
**J. M. C. Dos Santos**
University of Campinas - UNICAMP, Computational Mechanics Department, Rua Mendeleyev, 200, CEP13083-860, Campinas, SP, Brazil
zema@fem.unicamp.br

***Abstract.*** *The aim of the paper is to investigate the wave propagation and properties of periodicity on the frequency band structure of a circular cylindrical shell phononic cristal. The structural member is modelled using the semi-analytical technique called Spectral Element (SE) method, where the dynamic stiffness matrix of a circular cylindrical shell element is formulated. In the governing equations time derivatives are transformed by using the spectral decomposition, while the circumferential coordinate is eliminated by applying the solution in the form of Fourier series. By post-processing the SE model of a circular cylindrical shell unit-cell and applying the Floquet-Bloch theorem a transfer matrix eigenproblem is obtained, where the wave propagation behaviour along one-dimensional (1D) periodic systems can be calculated. This approach is called wave spectral element (WSE) method, and is also used to calculate band gaps in a circular cylindrical shell phononic crystal made with two elastic properties. Results are presented in frequency domain in dispersion diagrams. Precision and efficiency of the SE and WSE methods are demonstrated by computing wave propagation and band gaps in pipe like periodic structures with cylindrical shells spectral elements.*

***Keywords:*** *phononic crystal, spectral element, cylindrical shell*

## 1. INTRODUCTION

Shells have been used frequently as structural element in different areas of engineering applications. It comes from the fact that shells can be used for large span structures with good stiffness to weight ratio. Shells are subjected to various complex loading and boundary conditions, that can lead to structural failure, therefore, a good understanding of the dynamic behaviour of shell elements is very important to guarantee a safe and inexpensive design. Phononic crystals are artificial materials having discontinuities (inclusions, abrupt change of geometry or material property) which are periodically distributed along the space. Figure 1 shows an example of a phononic crystal cylindrical pipe made with two elastic material properties distributed periodically along its length, and a detail of the periodicity pattern (unit-cell). As a consequence of periodicity, those structures may exhibit frequency band gaps (stop or forbidden bands) where waves do not propagate. Based on this feature phononic crystals can be proposed as an efficient solution for vibration and noise control. Wave propagation in periodic structures has been extensively studied by many authors with origins that can be

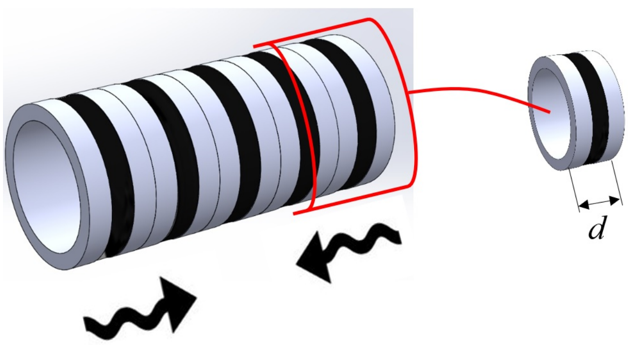


Figure 1: Scheme of a phononic crystal of circular cylindrical shells made with two materials: steel (silver) and polyacetal (black) distributed periodically along the length.

traced back to Newton and Rayleigh. The engineering study of periodic structures starts in the 70's with Mead, who wrote a good review about this subject in Mead (1996). The band gap phenomena in structural dynamics started to be analysed in the 90's, and one of the seminal works was written by Sigalas and Economou (1992). Since that, new approaches have appearing using periodicity together with analytical and numerical modelling to calculate complex structures at a low computational cost. One of these, also called wave spectral element (WSE) method, considers the spectral element (SE) model of a unit-cell the periodicity pattern expressed as a transfer matrix relation. Then, applying the Floquet-Bloch theorem an eigenvalue/vector transfer matrix problem is obtained, whose solution are the wave-numbers and wave modes which travel towards the right and left directions along the periodic structure. The WSE method has been applied to periodic structures built with element type like rods, beams and plates (Nobrega *et al.*, 2016; Silva and Arruda, 2012).

In the last decades many researches in phononic crystals and metamaterials had been done. From engineering point of view to analyse and understand these systems computationally and experimentally remains an open challenge (Hussein *et al.*, 2014). Phononic crystals produce band gaps, which are mostly induced by Bragg scattering effect (destructive interference of waves) generated by periodicity along a structure, for example, periodic changes in the elastic properties. For a 1D periodic structure with a unit-cell length $d$, band gaps would appear around frequencies governed by the Bragg condition, $d = n(\lambda/2), (n = 1, 2, \ldots)$ where $\lambda$ is the wavelength.

In this paper, the WSE method is applied to compute band gaps in a circular cylindrical shell whose elastic material properties vary along its length periodically (Figure 1). The motivation is to propose a new WSE approach based on the elastic circular cylindrical shell spectral element. Besides demonstrate that WSE method is accurate and efficient for modelling and simulating circular cylindrical shell phononic crystal. At first a comparative study for the cylindrical shell calculated by SE method and using the analytical solution (Leissa, 1973) is presented. The SE method consists in to obtain the govern equation exact solution for the circular cylindrical shell in a matrix form similar to the finite element (FE) method. In the governing equations time derivatives are transformed by using the spectral decomposition, while the circumferential coordinate is eliminated by applying the solution in the form of Fourier series (Kolarevic *et al.*, 2016). A two-end circular cylindrical shell spectral element with four degrees-of-freedom/end is obtained. The WSE method consists in post-processing the SE model of a circular cylindrical shell unit-cell and applying the Floquet-Bloch theorem to obtain a transfer matrix eigenproblem, where the wave propagation behaviour along 1D periodic systems is calculated. The WSE is used to analyse the wave propagation of a circular cylindrical shell phononic crystal. The method will be computationally implemented, verified and compared with the results obtained using a similar numerical approach, the wave finite element (WFE) method (Duhamel *et al.*, 2006; Mencik, 2014).

## 2. CIRCULAR CYLINDRICAL SHELL SPECTRAL ELEMENT

The SE method is based on the analytical solution of the displacement wave equation, written in the frequency domain (Doyle, 1997; Lee, 2004). The element is built in the concept of FE, but the form function is the exact solution of wave equation. Built-up structures with geometrically uniform members can be modelled by a single spectral element reducing significantly the total number of DOF's as compared to approximated approaches. However, there are still some drawbacks, such as, difficulties to model non-uniform members and elements without closed-form solution. For example, the free vibration problem of a rectangular plate, can be solved in closed-form only for a few combinations of boundary conditions. However, some spectral elements have been developed using approximations with superposition and Fourier series expansion (Casimir *et al.*, 2005; Campos and Arruda, 2007, 2008; Nefovska-Danilovic and Petronijevic, 2015; Kolarevic *et al.*, 2015). One in this category is the circular cylindrical shell spectral element developed by Kolarevic *et al.* (2016), which is applied here in WSE method. Its formulation will be briefly reviewed in this section.

The geometry (thickness $h$, radius $a$, length $L$) and coordinate system (displacements $u$, $v$ and $w$ of the mid surface in $x, \varphi$ and $z$ directions, respectively) for a closed circular cylindrical shell are is shown in Figure 2.

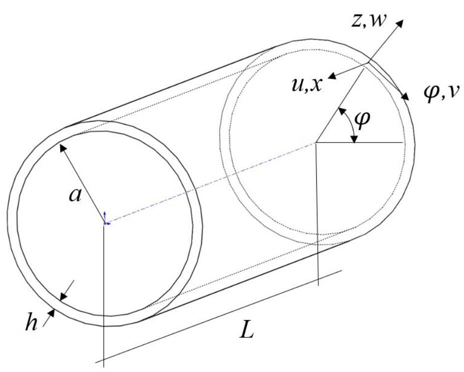


Figure 2: Geometry and coordinates system of a closed circular cylindrical shell.

Based on the Flügge thin shell theory (Leissa, 1973), the governing differential equations for a closed circular cylindrical shell can be written in a matrix form as:

$$\begin{bmatrix} \partial_x^2 + a_1\partial_\varphi^2 + a_2\partial_t^2 & a_3\partial_x\partial_\varphi & a_4\partial_x + a_5\partial_x^3 + a_6\partial_x\partial_\varphi^2 \\ a_3\partial_x\partial_\varphi & a_7\partial_\varphi^2 + a_8\partial_x^2 + a_2\partial_t^2 & a_7\partial_\varphi + a_9\partial_x^2\partial_\varphi \\ a_4\partial_x + a_5\partial_x^3 + a_6\partial_x\partial_\varphi^2 & a_7\partial_\varphi + a_9\partial_x^2\partial_\varphi & \begin{array}{c} k\left(\partial_x^4 + 2a_7\partial_x^2\partial_\varphi^2 + a_7{}^2\partial_\varphi^4\right) \\ + a_7 - a_2\partial_t^2 + 2a_{10}\partial_\varphi^2 + a_{10} \end{array} \end{bmatrix} \begin{bmatrix} u\left(x,\varphi,t\right) \\ v\left(x,\varphi,t\right) \\ w\left(x,\varphi,t\right) \end{bmatrix} = \begin{bmatrix} 0 \\ 0 \\ 0 \end{bmatrix} \tag{1}$$

where $u(x,\varphi,t)$, $v(x,\varphi,t)$ and $w(x,\varphi,t)$ denote displacement components in the axial ($x$), tangential ($\varphi$) and radial direction ($z$), respectively, and $\partial_x = d/dx$, $\partial_\varphi = d/d\varphi$, $\partial_t = d/dt$, and $k = h^2/12$. The $a_i (i = 1 \dots 10)$ coefficients of Eq. (1) are:

$$\begin{array}{lllll} a_1 = \frac{1-\nu}{2a^2}\left(1 + \frac{K}{Da^2}\right) & a_2 = \frac{\rho h}{D} \quad a_3 = \frac{1+\nu}{2a} & a_4 = \frac{\nu}{a} & a_5 = \frac{K}{Da} \\ a_6 = \frac{1-\nu}{2a^3}\frac{K}{D} & a_7 = \frac{1}{a^2} \quad a_8 = \frac{1-\nu}{2}\left(1 + \frac{3K}{Da^2}\right) & a_9 = \frac{3-\nu}{2}\frac{K}{Da^2} & a_{10} = \frac{K}{Da^4} \end{array} \tag{2}$$

where $\nu$ is the Poisson's ratio, $K = Eh^3/12(1-\nu^2)$ is the flexural stiffness, $D = Eh/(1-v^2)$ is the stiffness in the mid surface of shell, $\rho$ is the mass density and $E$ is the Young's modulus.

By using the separation of variables, the general solution of the system of Eq. (1) is:

$$u\left(x,\varphi,t\right) = \hat{u}\left(x,\varphi\right)e^{i\omega t}, \quad v\left(x,\varphi,t\right) = \hat{v}\left(x,\varphi\right)e^{i\omega t}, \quad w\left(x,\varphi,t\right) = \hat{w}\left(x,\varphi\right)e^{i\omega t} \tag{3}$$

where $\omega$ is the circular frequency and $\hat{u}, \hat{v}, \hat{w}$ are the spectral amplitude of displacement components. Substituting Eqs. (3) into Eqs. (1) the differential equation of circular cylindrical shell in frequency domain is obtained as:

$$\begin{bmatrix} \partial_x^2 + a_1\partial_\varphi^2 - a_2\omega^2 & a_3\partial_x\partial_\varphi & a_4\partial_x + a_5\partial_x^3 + a_6\partial_x\partial_\varphi^2 \\ a_3\partial_x\partial_\varphi & a_7\partial_\varphi^2 + a_8\partial_x^2 - a_2\omega^2 & a_7\partial_\varphi + a_9\partial_x^2\partial_\varphi \\ a_4\partial_x + a_5\partial_x^3 + a_6\partial_x\partial_\varphi^2 & a_7\partial_\varphi + a_9\partial_x^2\partial_\varphi & \begin{array}{c} k\left(\partial_x^4 + 2a_7\partial_x^2\partial_\varphi^2 + a_7{}^2\partial_\varphi^4\right) \\ + a_7 + a_2\omega^2 + 2a_{10}\partial_\varphi^2 + a_{10} \end{array} \end{bmatrix} \begin{bmatrix} \hat{u}\left(x,\varphi\right) \\ \hat{v}\left(x,\varphi\right) \\ \hat{w}\left(x,\varphi\right) \end{bmatrix} = \begin{bmatrix} 0 \\ 0 \\ 0 \end{bmatrix} \tag{4}$$

For a closed circular cylindrical shell, the displacement components $\hat{u}$ , $\hat{v}$ and $\hat{w}$ should satisfy periodicity in the tangential direction. Therefore, the solution of the system of Eqs. (4) can be expanded in an infinite Fourier series:

$$\begin{aligned} \hat{u}(x,\varphi) &= \sum_{m=0}^{\infty} U_m(x)\cos(m\varphi) + \sum_{m=1}^{\infty} U_m(x)\sin(m\varphi) \\ \hat{v}(x,\varphi) &= \sum_{m=0}^{\infty} V_m(x)\sin(m\varphi) + \sum_{m=1}^{\infty} V_m(x)\cos(m\varphi) \\ \hat{w}(x,\varphi) &= \sum_{m=0}^{\infty} W_m(x)\cos(m\varphi) + \sum_{m=1}^{\infty} W_m(x)\sin(m\varphi) \end{aligned} \tag{5}$$

where $m \in \mathbb{Z}$. Let's consider the case where the boundary conditions do not depend on $\varphi$. Then, the solutions for the different harmonics are uncoupled and instead of take the solution in the form of the summation, only the solution for the $m$-th harmonic will be considered. The solution for the asymmetric vibration ($m \geq 1$) will be presented, while the solution for the axisymmetric vibration ($m = 0$) will not be considered. The solution procedure for the 1st terms of Eqs.(5) will be presented, while the solution for the 2nd terms can be obtained in the same way. Notice that the natural frequencies obtained with the 1st and 2nd terms of Eqs. (5) are the same, which means that for the closed circular cylindrical shell all the natural frequencies are duplicated. By substituting the 1st terms of Eqs.(5) in the Eqs.(4) it has:

$$\begin{bmatrix} C_1\partial_x^2 + C_2 & C_3\partial_x & C_4\partial_x^3 + C_5\partial_x \\ -C_3\partial_x & C_6\partial_x^2 + C_7 & C_8\partial_x^2 + C_9 \\ C_4\partial_x^3 + C_5\partial_x & -C_8\partial_x^2 - C_9 & C_{10}\partial_x^4 + C_{11}\partial_x^2 + C_{12} \end{bmatrix} \begin{bmatrix} \hat{u}\left(x\right) \\ \hat{v}\left(x\right) \\ \hat{w}\left(x\right) \end{bmatrix} = \begin{bmatrix} 0 \\ 0 \\ 0 \end{bmatrix} \tag{6}$$

where

$$
\begin{array}{llll}
C_{1,m} = 1 & C_{2,m} = -m^2 a_1 - w^2 a_2 & C_{3,m} = -m a_3 & C_{4,m} = -a_5 \\
C_{5,m} = a_4 - m^2 a_6 & C_{6,m} = a_8 & C_{7,m} = -m^2 a_7 - w^2 a_2 & C_{8,m} = -m a_9 \\
C_{9,m} = -m a_7 & C_{10,m} = k & C_{11,m} = -2km^2 a_7 & \begin{array}{l} C_{12,m} = -a_7 + w^2 a_2 \\ + k(m^4 a_7^2 - 2m^2 a_7 + a_7^4) \end{array}
\end{array}
\tag{7}
$$

By expanding the determinant of the matrix of Eqs. (6), an 8th order differential equation is obtained as:

$$
(\partial_x^8 + a_{1,m}\partial_x^6 + a_{2,m}\partial_x^4 + a_{3,m}\partial_x^2 + a_{4,m}\partial_x)\Psi = 0 \tag{8}
$$

where $\Psi = U_m$ or $V_m$ or $W_m$, and:

$$
\begin{aligned}
a_{1,m} &= \tfrac{c_{10}c_3^2 + 2c_3c_4c_8 - c_7c_4^2 - 2c_5c_6c_4 + c_1c_8^2 + c_1c_6c_{11} + c_1c_7c_{10} + c_2c_6c_{10}}{c_1c_6c_{10} - c_6c_4^2} \\
a_{2,m} &= \tfrac{c_1c_6c_{12} + c_{11}c_3^2 + 2c_3c_5c_8 + 2c_4c_9c_3 - c_6c_5^2 - 2c_4c_7c_5 + c_2c_8^2 + 2c_1c_9c_8 + c_1c_7c_{11} + c_2c_6c_{11} + c_2c_7c_{10}}{c_1c_6c_{10} - c_6c_4^2} \\
a_{3m} &= \tfrac{c_{12}c_3^2 + 2c_3c_5c_9 - c_7c_5^2 + c_1c_9^2 + 2c_2c_8c_9 + c_1c_7c_{12} + c_2c_6c_{12} + c_2c_7c_{11}}{c_1c_6c_{10} - c_6c_4^2}; \\
a_{4,m} &= \tfrac{c_* c_9^2 + c_2c_7c_12}{c_1c_6c_{10} - c_6c_4^2}
\end{aligned}
\tag{9}
$$

Assuming the solution of the Eq. (8) in the form $\Psi = e^{rx}$ the corresponding characteristic equation is obtained as:

$$
r^8 + a_{1,m}r^6 + a_{2,m}rx^4 + a_{3,m}r^2 + a_{4,m}r = 0 \tag{10}
$$

whose roots are $r_{i,m}(i = 1, \dots, 8)$. The solutions for unknown functions can be written as:

$$
U_m(x) = \sum_{i=1}^{\infty} A_{i,m}e^{r_{i,m}x}; \quad V_m(x) = \sum_{i=1}^{\infty} B_{i,m}e^{r_{i,m}x}; \quad W_m(x) = \sum_{i=1}^{\infty} C_{i,m}e^{r_{i,m}x} \tag{11}
$$

where from a total of 24 integration constants only 8 are independent. The integration constants $A_{i,m}$, and $B_{i,m}$, can be expressed in terms of $C_{i,m}$ by doing

$$
A_{i,m} = \delta_{i,m}C_{i,m}; \quad B_{i,m} = \gamma_{i,m}C_{i,m} \tag{12}
$$

where $\delta_{i,m}$, and $\gamma_{i,m}$, are coefficients that represent amplitude the ratios of axial-radial and tangential-radial displacements, respectively:

$$
\delta_{i,m} = \frac{(c_9 + c_8r_i^2)^2 + (c_7 + c_6r_i^2)(c_{12} + c_{11}r_i^2 + c_{10}r_i^4)}{r_i(c_5 + c_4r_i^2)(c_7 + c_6r_i^2) - c_3r_i(c_9 + c_8r_i^2)} \tag{13}
$$

$$
\gamma_{i,m} = \frac{(c_{12}c_3 + c_5c_9 + (c_{11}c_3 + c_5c_8 + c_4c_9)(r_i^2) + (c_10c_3 + c_4c_8)r_i^4)}{(c_5c_7 - c_3c_9 + (c_5c_6 + c_4c_7 - c_3c_8)(r_i^2) + c_4c_6r_i^4)} \tag{14}
$$

Substituting the Eqs.(11) and (12) in the Eqs.(5), keeping only the 1st terms and truncating the summation index as $m = 1, \dots, M$ the displacement components can be written as:

$$
\begin{aligned}
\hat{u}(x,\varphi) &= \sum_{m=1}^{M}\left(\sum_{i=1}^{8}\delta_{i,m}C_{i,m}e^{r_{i,m}x}\right)\cos(m\varphi) \\
\hat{v}(x,\varphi) &= \sum_{m=1}^{M}\left(\sum_{i=1}^{8}\gamma_{i,m}C_{i,m}e^{r_{i,m}x}\right)\sin(m\varphi) \\
\hat{w}(x,\varphi) &= \sum_{m=1}^{M}\left(\sum_{i=1}^{8}C_{i,m}e^{r_{i,m}x}\right)\cos(m\varphi)
\end{aligned}
\tag{15}
$$

As a matter of conciseness the equations of force and moments for the circular cylindrical shell are not presented in the paper, but can be founded in (Leissa, 1973). By substituting Eqs. (15) in these equations the expressions for forces and moments in frequency domain can be obtained.

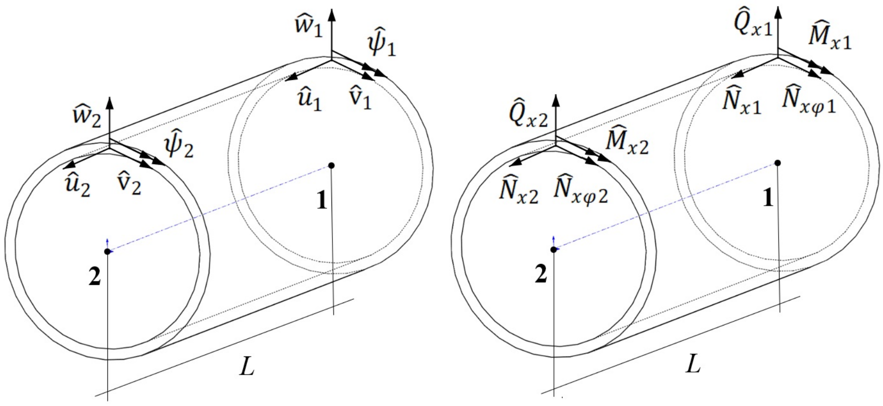


Figure 3: Two-end circular cylindrical shell spectral element with components of the displacement (*left*) and the force (*right*) vectors.

Figure 3 shows schemes of two-end circular cylindrical shell spectral element of length $L$ including components of the displacement (*left*) and the force (*right*) vectors. By defining the displacement vector $\hat{q}$ containing the displacements and rotations at the element ends $x = 0$ and $x = L$ it has:

$$\hat{q} = [\hat{u}_1 \ \hat{v}_1 \ \hat{w}_1 \ \hat{\psi}_{\varphi 1} \ \hat{u}_2 \ \hat{v}_2 \ \hat{w}_2 \ \hat{\psi}_{\varphi 2}]^T \tag{16}$$

where

$$\begin{array}{ll} \hat{u}_1 = \hat{u}(0,\varphi) = U_m(0)\cos(m\varphi); & \hat{u}_2 = \hat{u}(L,\varphi) = U_m(L)\cos(m\varphi); \\ \hat{v}_1 = \hat{v}(0,\varphi) = \hat{v}(0,\varphi) = V_m(0)\sin(m\varphi); & \hat{v}_2 = \hat{v}(L,\varphi) = \hat{v}(L,\varphi) = V_m(L)\sin(m\varphi); \\ \hat{w}_1 = \hat{w}(0,\varphi) = \hat{w}(0,\varphi) = W_m(0)\cos(m\varphi); & \hat{w}(L,\varphi) = \hat{w}(L,\varphi) = W_m(L)\cos(m\varphi); \\ \hat{\psi}_{\varphi 1} = \hat{\psi}_\varphi(0,\varphi) = \hat{\psi}_\varphi(0,\varphi) = \Psi_m(0)\cos(m\varphi); & \hat{\psi}_{\varphi 2}(L,\varphi) = \hat{\psi}_\varphi(L,\varphi) = \Psi_m(L)\cos(m\varphi) \\ \hat{\psi}_\varphi(x,\varphi) = \frac{\partial \hat{w}(x,\varphi)}{\partial x} & \end{array} \tag{17}$$

Similarly for the force vector,

$$\hat{Q} = [\hat{N}_{x1} \ \hat{N}_{x\varphi 1} \ \hat{Q}_{x1} \ \hat{M}_{x1} \ \hat{N}_{x2} \ \hat{N}_{x\varphi 2} \ \hat{Q}_{x2} \ \hat{M}_{x2}]^T \tag{18}$$

where $\hat{N}_{x1} = -\hat{N}_x(0,\varphi), \hat{N}_{x\varphi 1} = -\hat{N}_{x\varphi}(0,\varphi), \hat{Q}_{x1} = -\hat{Q}_x(0,\varphi), \hat{M}_{x1} = -\hat{M}_x(0,\varphi), \hat{N}_{x2} = \hat{N}_x(L,\varphi), \hat{N}_{x\varphi 2} = \hat{N}_{x\varphi}(L,\varphi), \hat{Q}_{x2} = \hat{Q}_x(L,\varphi)$, and $\hat{M}_{x2} = \hat{M}_x(L,\varphi)$ with the nodal forces and moments given by (Kolarevic *et al.*, 2016):

$$\hat{N}_{x(i,m)}(x,\varphi) = \frac{(D\nu(1 + m\gamma_{i,m}) + aDr_{i,m}\delta_{i,m} - Kr_{i,m}^2}{a} \tag{19}$$

$$\hat{N}_{x\varphi(i,m)}(x,\varphi) = \frac{(1-\nu)[-aD\delta_{i,m}m + a^2 D\gamma_{i,m}r_{i,m} + 3Kr_{i,m}(\gamma_{i,m} + m)]}{2a^2} \tag{20}$$

$$\hat{Q}_{x(i,m)}(x,\varphi) = \frac{K[(1-\nu)\delta_{i,m}m^2 + 2a^2 r_{i,m}^2(\delta_{i,m} - ar_{i,m})]}{2a^3} + \frac{Kmr_{i,m}[(3-\nu)\gamma_{i,m} + 2m(2-\nu)]}{2a^2} \tag{21}$$

$$\hat{M}_{x(i,m)}(x,\varphi) = \frac{K[m\nu(\gamma_{i,m} + m) + ar_{i,m}\delta_{i,m} - a^2 r_{i,m}^2]}{a^2} \tag{22}$$

The new displacement and force vector, namely $\hat{\mathbf{q}}_m$, that contain the amplitudes of displacements and rotations, and $\hat{\mathbf{Q}}_m$ that include the amplitudes of forces and moments, both on the boundaries $x = 0$ and $x = L$ for the $m$-th harmonic are:

$$\hat{\mathbf{q}}_m = [U_m(0) \ V_m(0) \ W_m(0) \ \Psi_{\varphi m}(0) \ U_m(L) \ V_m(L) \ W_m(L) \ \Psi_{\varphi m}(L)]^T \tag{23}$$

$$\hat{\mathbf{Q}}_m = [-\hat{N}_{xm}(0) \ -\hat{N}_{x\varphi m}(0) \ -\hat{Q}_{xm}(0) \ -\hat{M}_{xm}(0) \ +\hat{N}_{xm}(L) \ +\hat{N}_{x\varphi m}(L) \ +\hat{Q}_{xm}(L) \ +\hat{M}_{xm}(L)]^T \tag{24}$$

The vector $\hat{\mathbf{q}}_m$ is related to the vector of integration constants $\mathbf{C}_m$ by the matrix $\mathbf{D}_m$ , while the vectors $\hat{\mathbf{Q}}_m$ and $\mathbf{C}_m$ are related through the matrix $\mathbf{F}_m$ , as follows:

$$\hat{\mathbf{q}}_m = \mathbf{D}_m\mathbf{C}_m \tag{25}$$

$$\hat{\mathbf{Q}}_m = \mathbf{F}_m \mathbf{C}_m \tag{26}$$

where the vector of integration constants $\mathbf{C}_m$ and the matrices $\mathbf{D}_m$ and $\mathbf{F}_m$ are:

$$\mathbf{C}_m = [C_{1,m}\ C_{2,m}\ C_{3,m}\ C_{4,m}\ C_{5,m}\ C_{6,m}\ C_{7,m}\ C_{8,m}]^T \tag{27}$$

$$\mathbf{D}_m = \begin{bmatrix} \delta_{1,m} & \cdots & \delta_{8,m} \\ \gamma_{i,m} & \cdots & \gamma_{i,m} \\ 1 & \cdots & 1 \\ -r_{1,m} & \cdots & -r_{8,m} \\ \delta_{1,m}e^{r_{i,m}L} & \cdots & \delta_{8,m}e^{r_{8,m}L} \\ \gamma_{i,m}e^{r_{i,m}L} & \cdots & \gamma_{i,m}e^{r_{i,m}L} \\ e^{r_{i,m}L} & \cdots & e^{r_{i,m}L} \\ -r_{1,m}e^{r_{i,m}L} & \cdots & -r_{8,m}e^{r_{i,m}L} \end{bmatrix} \mathbf{F}_m = \begin{bmatrix} -\hat{N}_{x(1,m)} & \cdots & -\hat{N}_{x(8,m)} \\ -\hat{N}_{x\varphi(1,m)} & \cdots & -\hat{N}_{x\varphi(8,m)} \\ -\hat{Q}_{x(1,m)} & \cdots & -\hat{Q}_{x(8,m)} \\ -\hat{M}_{x(1,m)} & \cdots & -\hat{M}_{x(8\mathrm{m})} \\ \hat{N}_{x(1,m)}e^{r_{i,m}L} & \cdots & \hat{N}_{x(8,m)}e^{r_{8,m}L} \\ \hat{N}_{x\varphi(1,m)}e^{r_{i,m}L} & \cdots & \hat{N}_{x\varphi(8,m)}e^{r_{8,m}L} \\ \hat{Q}_{x(1,m)}e^{r_{i,m}L} & \cdots & \hat{Q}_{x(8,m)}e^{r_{8,m}L} \\ \hat{M}_{x(1,m)}e^{r_{i,m}L} & \cdots & \hat{M}_{x(8\mathrm{m})}e^{r_{8,m}L} \end{bmatrix} \tag{28}$$

If vector $\mathbf{C}_m$ is expressed from the Eqs. (25) as a function of $\hat{\mathbf{q}}_m$ and replaced in the Eq. (26), the relation between vectors $\hat{\mathbf{Q}}_m$ and $\hat{\mathbf{q}}_m$ is obtained in the following form:

$$\hat{\mathbf{Q}}_m = \mathbf{K}_{Dm} \hat{\mathbf{q}}_m \tag{29}$$

where $\mathbf{K}_{Dm} = \mathbf{F}_m(\mathbf{D}_m)^{-1}$ is the dynamic stiffness matrix of the circular cylindrical shells spectral element for the $m$-th harmonic.

## 3. PHONONIC CRYSTAL MODELLING BY WSE & WFE METHOD

Consider an elastic phononic crystal circular cylindrical shell with spatial periodic distribution with a unit-cell length $d$, as sketched in Fig. 1. For the spatial periodic distribution the band gaps are generated by Bragg scattering, which appears around frequencies governed by the Bragg condition $d = n(\lambda/2)(n = 1, 2, \ldots)$, where $\lambda$ is the unit-cell wavelength. In this paper two circular cylindrical shell models are used: one is formulated with the semi-analytical SE method presented in Section 2, and the other is the approximated numeric conventional FE method (Cook *et al.*, 1974). The equilibrium equation for the finite circular cylindrical shell by SE is given by the Eq. (29) with the spectral dynamic stiffness element matrix rewritten here as:

$$\mathbf{D}_{se} = \mathbf{F}_m(\mathbf{D}_m)^{-1} \tag{30}$$

where the matrices $\mathbf{F}_m$ and $\mathbf{D}_m$ are given by Eqs.(28).

The dynamic stiffness element matrix by FE method can be written as:

$$\mathbf{D}_{fe} = \mathbf{K}_{fe} - \omega^2 \mathbf{M}_{fe} \tag{31}$$

where $\mathbf{K}_{fe}$ and $\mathbf{M}_{fe}$ are the conventional finite element circular cylindrical shell stiffness and mass matrices, respectively, not shown here in detail, but can be found in Cook *et al.* (1974). The dynamic stiffness matrix, either by SE or FE, can be partitioned in terms of internal, left-sided and right-sided degrees of freedom by

$$\begin{bmatrix} \mathbf{D}_{ii} & \mathbf{D}_{il} & \mathbf{D}_{ir} \\ \mathbf{D}_{li} & \mathbf{D}_{ll} & \mathbf{D}_{lr} \\ \mathbf{D}_{ri} & \mathbf{D}_{rl} & \mathbf{D}_{rr} \end{bmatrix} \begin{Bmatrix} \hat{\mathbf{q}}_i \\ \hat{\mathbf{q}}_l \\ \hat{\mathbf{q}}_r \end{Bmatrix} = \begin{Bmatrix} \mathbf{0}_i \\ \hat{\mathbf{Q}}_l \\ \hat{\mathbf{Q}}_r \end{Bmatrix} \tag{32}$$

From Eq. 32, the internal displacement vector can be obtained as

$$\hat{\mathbf{q}}_i = \mathbf{D}_{ii}^{-1} \left( \mathbf{D}_{il} \hat{\mathbf{q}}_l + \mathbf{D}_{ir} \hat{\mathbf{q}}_r \right) \tag{33}$$

Substituting Eq.33 into Eq. 32, the condensed dynamic stiffness matrix is obtained as

$$\begin{bmatrix} \mathbf{D}_{ll} & \mathbf{D}_{lr} \\ \mathbf{D}_{rl} & \mathbf{D}_{rr} \end{bmatrix} \begin{Bmatrix} \hat{\mathbf{q}}_l \\ \hat{\mathbf{q}}_r \end{Bmatrix} = \begin{Bmatrix} \hat{\mathbf{Q}}_l \\ \hat{\mathbf{Q}}_r \end{Bmatrix} \tag{34}$$

where $\mathbf{D}_{ll} = \mathbf{D}_{ll} - \mathbf{D}_{li}\mathbf{D}_{ii}^{-1}\mathbf{D}_{il}$, $\mathbf{D}_{rl} = \mathbf{D}_{rl} - \mathbf{D}_{ri}\mathbf{D}_{ii}^{-1}\mathbf{D}_{il}$, $\mathbf{D}_{lr} = \mathbf{D}_{lr} - \mathbf{D}_{li}\mathbf{D}_{ii}^{-1}\mathbf{D}_{ir}$ and $\mathbf{D}_{rr} = \mathbf{D}_{rr} - \mathbf{D}_{ri}\mathbf{D}_{ii}^{-1}\mathbf{D}_{ir}$.

The periodicity condition allows predicting the behavior under harmonic disturbance of a periodic system modelling a unit-cell only. In this method the dynamic stiffness matrix of a unit-cell modelled by SE or FE is used to apply the periodicity condition in a harmonic disturbance propagating through the system. Using Floquet-Bloch's theorem, the periodicity condition results in an eigenvalue problem. Equation 34 can be rearranged in a the Transfer Matrix formulation, resulting in

$$\underbrace{\begin{Bmatrix} \hat{\mathbf{q}}_r \\ -\hat{\mathbf{Q}}_r \end{Bmatrix}}_{\mathbf{p}_r} = \underbrace{\begin{Bmatrix} -\mathbf{D}_{lr}^{-1}\mathbf{D}_{ll} & -\mathbf{D}_{lr}^{-1} \\ \mathbf{D}_{rl} - \mathbf{D}_{rr}\mathbf{D}_{lr}^{-1}\mathbf{D}_{ll} & -\mathbf{D}_{rr}^{-1}\mathbf{D}_{lr} \end{Bmatrix}}_{\mathbf{T}} \underbrace{\begin{Bmatrix} \hat{\mathbf{q}}_l \\ \hat{\mathbf{Q}}_l \end{Bmatrix}}_{\mathbf{p}_l} \tag{35}$$

where $\mathbf{T}$ is the transfer matrix that relates the left state vector $\mathbf{p}_l$ with the right state vector $\mathbf{p}_r$ of the unit-cell.

Considering now consecutive unit-cells, *m* and *m*+1, results

$$\mathbf{p}_l^{(m+1)} = \mathbf{T}\mathbf{p}_l^{(m)} \tag{36}$$

For wave propagation in an infinite periodic system, Floquet-BlochâĂŹs theorem produces an eigenvalue problem given by

$$\mathbf{T}\mathbf{p}_l = e^{\mu}\mathbf{p}_l \tag{37}$$

where $e^{\mu}$ is the eigenvalue, $\mathbf{p}_l$ is the eigenvector, $\mu = -ikd$ is the attenuation constant, where $d$ is the unit-cell length, $k$ is the wavenumber and $i$ is the imaginary unit. This solution provides the behavior in terms of wave propagation.

## 4. NUMERICAL RESULTS

To verify the implementation of the circular cylindrical shell spectral element simulated examples are performed. A circular cylindrical shell of thickness $h = 0.01m$, radius $a = 1.0m$, length $L = 20m$, made of steel with mass density $\rho = 7850kg/m^3$, Poisson's ratio $\nu = 0.3$ and Young Modulus$E = 210 \times 10^9 N/m^3$ is used. A theoretical modal analysis using SE method implemented in a MATLAB code is carry out and 10 lowest natural frequencies are calculated. These results are compared with that calculated by FE method in the commercial software ANSYS, using element type SHELL63 (6 DOF's/node) and the circular cylindrical shell is discretized with 7201 elements and 7321 nodes. The modal analysis were performed using two different boundary conditions in the cylindrical shell-ends: clamped-clamped and free-free. Table 1 shows the results for a clamped-clamped (C-C) and free-free (F-F) boundary conditions including the mode number, natural frequencies calculated by FE and SE and the percentage relative error. It can be seen that for both boundary conditions (C-C and F-F) the natural frequency relative errors between FE and SE are very small, with the highest value of 0.45 % for C-C and 4.61 % for F-F. Of course, that this values are dependent of the FE model discretization and errors even lower can be reached by using finer meshing.

Table 1: Natural frequency of a circular cylindrical shell by FE and SE methods.

| B. Conditions | Order | Mode Number $(m, n)$ | FE (Hz) | SE (Hz) | R. Error $\%$ |
|---|---|---|---|---|---|
| Clamped-Clamped | 1 | (2,1) | 11.99 | 12.03 | 0.33 |
| | 2 | (3,1) | 19.54 | 19.58 | 0.20 |
| | 3 | (3,2) | 23.08 | 23.17 | 0.38 |
| | 4 | (2,2) | 27.18 | 27.22 | 0.14 |
| | 5 | (1,1) | 28.31 | 28.30 | 0.03 |
| | 6 | (3,3) | 31.48 | 31.59 | 0.34 |
| | 7 | (4,1) | 36.36 | 36.43 | 0.19 |
| | 8 | (4,2) | 37.21 | 37.24 | 0.08 |
| | 9 | (4,3) | 39.52 | 39.70 | 0.45 |
| | 10 | (4,4) | 44.10 | 44.27 | 0.38 |
| Free-Free | 1 | (2,1) | 6.68 | 6.69 | 0.14 |
| | 2 | (2,2) | 12.25 | 12.13 | 0.98 |
| | 3 | (3,1) | 18.88 | 18.92 | 0.21 |
| | 4 | (3,2) | 19.67 | 19.61 | 0.30 |
| | 5 | (3,3) | 23.40 | 23.26 | 0.60 |
| | 6 | (2,3) | 28.27 | 27.65 | 2.24 |
| | 7 | (1,1) | 30.63 | 29.28 | 4.61 |
| | 8 | (3,4) | 32.19 | 31.85 | 1.06 |
| | 9 | (4,1) | 36.19 | 36.38 | 0.52 |
| | 10 | (4,2) | 37.48 | 37.25 | 0.61 |

In order to validate the WSE approach a unit-cell with $d = 0.2$m of an homogeneous circular cylindrical shell, using the same geometry and elastic properties of the former example was simulated. Dispersion diagrams are calculated and compared with that obtained by analytical solution given by **?**. Figure 4 shows the dispersion curves calculated by WSE approach and Analytical solution for the harmonic modes $m = 1$ and $m = 2$. It can be seen a very good agreement between both methods at low frequency bands, but as the frequency band increase they start to diverge. It comes from the fact that WSE circular cylindrical shell model is based on Flügge's shell theory, while the analytical solution of **?** model is formulated using the Donnell-Musthari's shell theory, which is more conservative.

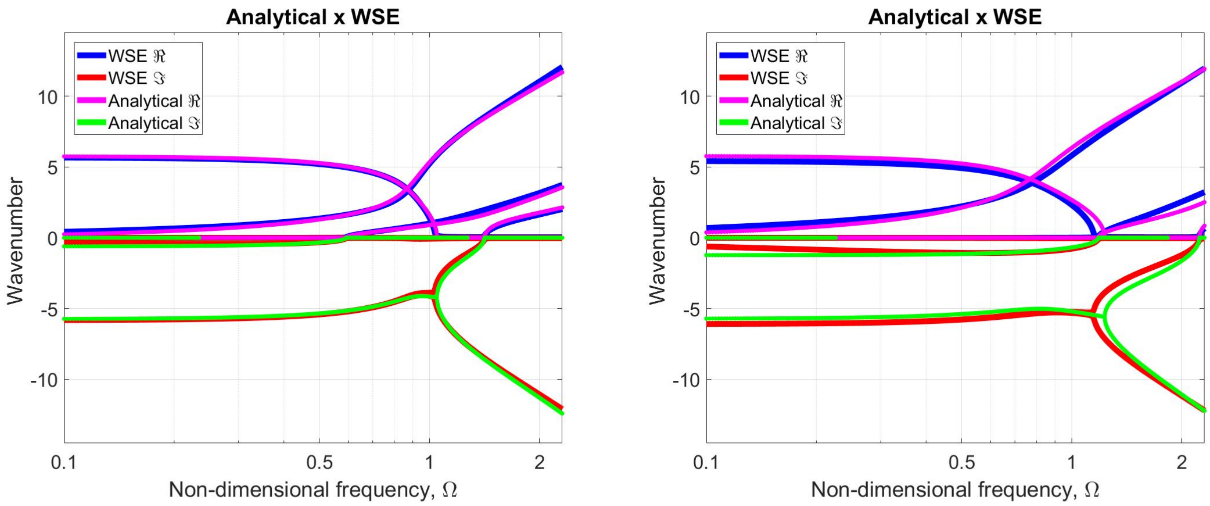


($a$) ($b$)

Figure 4: Dispersion diagram calculated by analytical and WSE methods for the harmonic: ($a$) $m = 1$; ($b$) $m = 2$.

To WSE is also evaluate to obtain the band gaps in a phononic crystal of a circular cylindrical shell. A phononic crystal circular cylindrical shell unit-cell is made with two materials combined as steel-polyacetal-steel (Figure 1) with thickness $h = 0.025m$, radius $a = 0.05m$, steel unit-cell length $d_1 = 0.01m$ and polyacetal unit-cell length $d_2 = 0.03m$. Steel properties are mass density $\rho_s = 8030kg/m^3$, Poisson's ratio $\nu_s = 0.27$ and Young Modulus$E_s = 193 \times 10^9 N/m^3$. Poyacetal properties are mass density $\rho_p = 1418kg/m^3$, Poisson's ratio $\nu_p = 0.35$ and Young Modulus $E_p = 3.3 \times 10^9 N/m^3$. Figure 5 presents the dispersion diagram for the phononic crystal calculated by WSE and WFE (Sousa *et al.*, 2017) for the harmonic mode $m = 0$. It can be seen a good agreement between the curves at low frequency bands, but as the frequency increases they starts to diverge. This behaviour is related with sizing mesh of WFE method, which can be improved increasing the size meshing. For others harmonic modes (not shown here) a similar behaviour was founded.

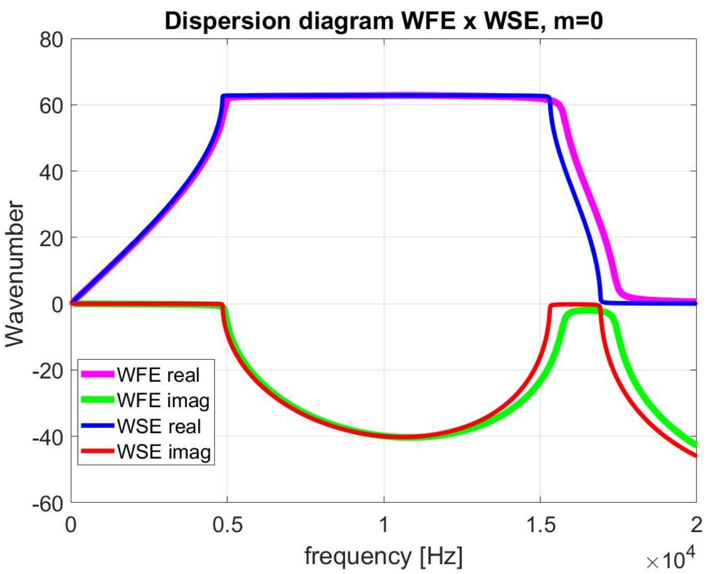


Figure 5: Dispersion diagram of phononic crystal circular cylindrical shell calculated by WSE and WFE for the harmonic mode $m = 0$.

Figure 6 shows the dispersion diagrams calculated for the harmonic modes $m = 1 \ldots 4$. It can be seen that for all harmonics mode the method can identify the band gaps as expected. This results corroborates that WSE method is able to identify the locations and widths of band gaps, which occur at the locations where the imaginary part of the wavenumber becomes negative (evanescent wave) in the dispersion diagram.

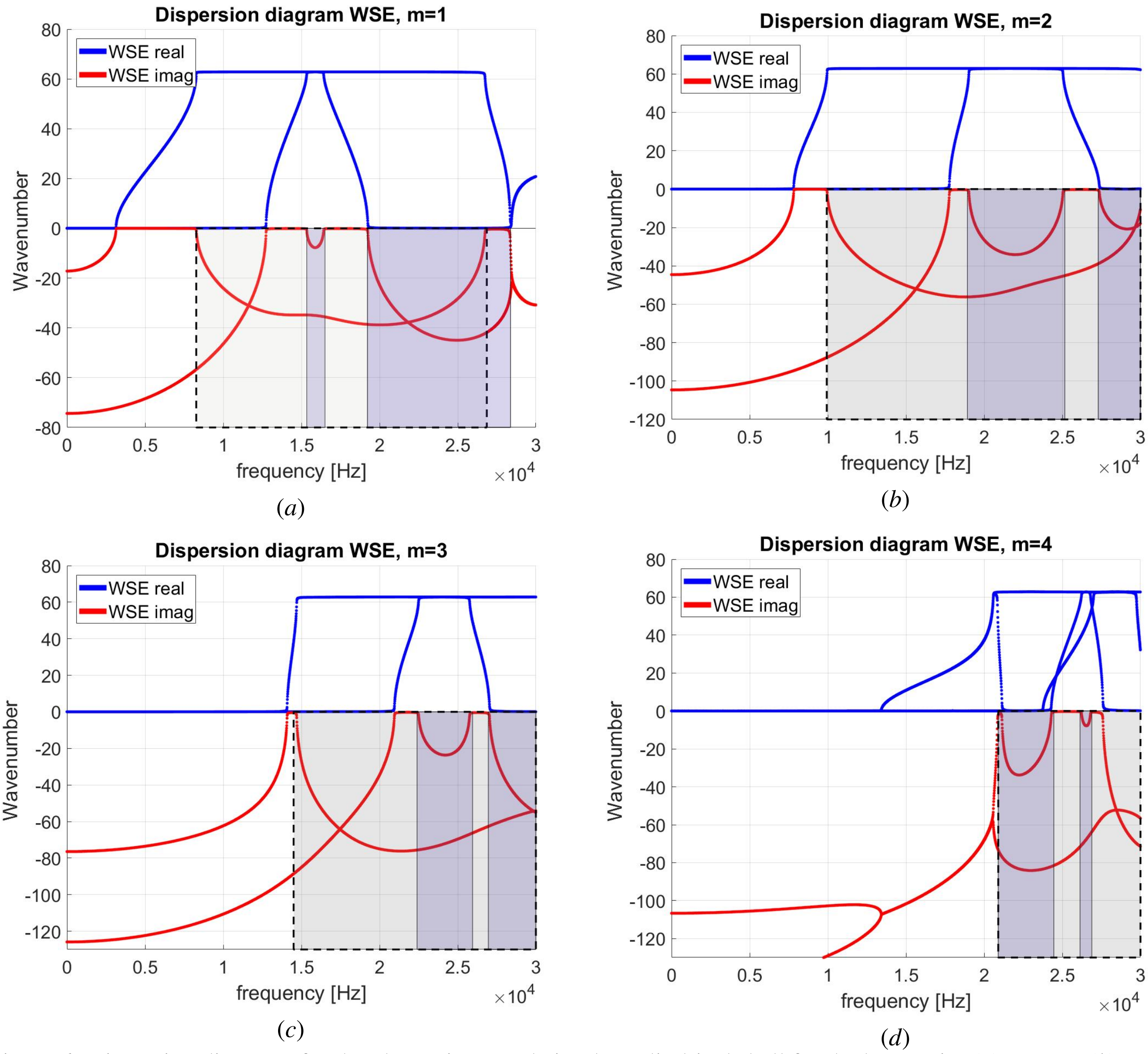


Figure 6: Dispersion diagrams for the phononic crystal circular cylindrical shell for the harmonic: (*a*) $m = 1$; (*b*) $m = 2$; (*c*) $m = 3$; (*d*) $m = 4$.

## 5. CONCLUSION

The WSE method have been considered and implemented to compute the wave modes in free-free homogeneous and phononic crystal circular cylindrical shells. The accuracy of the circular cylindrical shell spectral element has been clearly demonstrated. Also, the WSE approach constitutes a relevant numerical tool which is capable of predicting band gaps locations and widths in the dispersion diagrams of phononic crystal structures. Of course, these are preliminary results and others verifications are under way related with the efficiency and harmonic response using the WSE method.

## 6. ACKNOWLEDGEMENTS

The authors are thankful to CAPES Dinter-UEMA-UNICAMP for the financial support.

## 7. REFERENCES

Campos, N. and Arruda, J., 2007. “Modeling Kirchhoff plates with arbitrary boundary conditions by the spectral element method”. In *Proceedings of the XII International Symposium on Dynamic Problems of Mechanics (XII DINAME)*.

Campos, N. and Arruda, J., 2008. "On the modeling of beam reinforced thin plates using the spectral element method". *Shock and Vibration*, , No. 15, pp. 425–434.

Casimir, J., Kevorkian, S. and Vinh, T., 2005. "The dynamic stiffness matrix of two- dimensional elements: application to Kirchhoff's plate continuous elements". *Journal of Sound and Vibration*, Vol. 287, No. 3, pp. 571–589. doi: 10.1016/j.jsv.2004.11.013.

Cook, R., Malkus, D., Plesha, M. and Witt, R., 1974. *Concepts and Applications of Finite Element Analysis*. John Wiley and Sons, New York, US, st edition edition.

Doyle, J.F., 1997. *Wave propagation in structures : spectral analysis using fast discrete Fourier transforms*. Mechanical engineering. Springer-Verlag New York, Inc., New York, 2nd edition.

Duhamel, D., Mace, B.R. and Brennan, M.J., 2006. "Finite element analysis of the vibrations of waveguides and periodic structures". *Journal of Sound and Vibration*, Vol. 294, No. 1-2, pp. 205–220.

Hussein, M., Leamy, M. and Ruzzene, M., 2014. "Dynamics of phononic materials and structures: Historical origins, recent progress, and future outlook". Vol. 66, p. 040802.

Kolarevic, N., Nefovska-Danilovic, M. and Petronijevic, M., 2015. "Dynamic stiffness elements for free vibration analysis of rectangular mindlin plate assemblies." *Journal of Sound and Vibration*, Vol. 359, No. 12, pp. 84–106. doi: 10.1016/j.jsv.2015.06.031.

Kolarevic, N., Nefovska-Danilovic, M. and Petronijevic, M., 2016. "Dynamic stiffness method in the vibration analysis of circular cylindrical shell". Vol. 59, pp. 45–61.

Lee, U., 2004. *Spectral Element Method in Structural Dynamics*. BInha University Press.

Leissa, A.W., 1973. *Vibration of shells*. Government Printing Office, Washington, D.C., US, 1st edition.

Mead, D.J., 1996. "Wave propagation in continuous periodic structures. research contributions from southampton". *Journal of Sound and Vibration*, Vol. 190, pp. 495–524.

Mencik, J.M., 2014. "New advances in the forced response computation of periodic structures using the wave finite element (WFE) method". *Computational Mechanics*, Vol. 54, No. 3, pp. 789–801.

Nefovska-Danilovic, M. and Petronijevic, M., 2015. "In-plane free vibration and response analysis of isotropic rectangular plates using the dynamic stiffness method". *Computers and Structures*, Vol. 152, No. 5, pp. 82–95. doi: 10.1016/j.compstruc.2015.02.001.

Nobrega, E.D., Gautier, F., Pelat, A. and Dos Santos, J.M.C., 2016. "Vibration bandgaps for elastic metamaterial rods using wave finite element method". *Mechanical Systems and Signal Processing*, Vol. 79, pp. 192–202.

Sigalas, M.M. and Economou, E.N., 1992. "Elastic and acoustic wave band structure". *Journal of Sound and Vibration*, Vol. 158, pp. 377–382.

Silva, P.B. and Arruda, J.R.F., 2012. "Wave spectral finite element analysis of two-dimensional waveguides". In *Proceedings of the Eleventh International Conference on Computational Structures Technology*. Stirlingshire, Scotland.

Sousa, R., Mencik, J.M. and Dos Santos, J., 2017. "Band gaps in plates and cylindrical shells with 1d periodic elastic properties". In *Proceedings of the 24th International Congress of Mechanical Engineering*. Curitiba, PR, Brazil.

## 8. RESPONSIBILITY NOTICE

The authors are the only responsible for the printed material included in this paper.